Supporting Information

Tailoring the π-π stacking interaction among 2,3'-bipyridine molecules in hybrid metal halide crystals towards tunable light emitting

Qi Zhang,[a] Xinyi Lin, [a] Shanji Guo,[b] Yaqing Zhang,[a] Yan Jiang,[a] Wei Zhang,[a] Hui Li,[a] Ya-Nan Feng,[a] Lingyun Li,*[a] Zheyuan Liu,*[a] and Yan Yu*[a]

[a] Q. Zhang, X. Lin, Y. Zhang, Y. Jiang, W. Zhang, H. Li and Y.-N. Feng
Key Laboratory of Advanced Materials Technologies, International (HongKong Macao and Taiwan) Joint Laboratory on Advanced Materials Technologies, College of Materials Science and Engineering, Fuzhou University, No.2 Wu Long Jiang North Avenue, Fuzhou, Fujian, 350108, China
E-mail: lilingyun@fzu.edu.cn, zheyuan.liu@fzu.edu.cn, yuyan@fzu.edu.cn
[b] S. Guo
Fuyao Industrial Area II, Fuyao Glass Industry Group Co., Ltd., Fuqing, Fujian, 350301, China

Content

1. Materials and methods

Analytically pure 2,3'-bipyridine, $CdCl_2$, $ZnCl_2$ and hydrochloric acid were purchased from the Shanghai Macklin Biochemical Co. Ltd. and used without further purification.

1.1 Synthesis of 23-CdCl compound

$CdCl_2$ (0.05 mmol) and HCl (3 mmol) were dissolved in mixed solution in H_2O (3 mL) and 2,3'-bipyridine (1 mL), and the mixture was then in a 25 mL round bottom flask reactor. The reactor was first heated at 80 °C for 3 hours and then slowly cooled to room temperature with a cooling rate of 5 °C·min^{-1}. After the filtration, block-shaped colorless crystals were obtained and subsequently determined as 23-CdCl. After crystal structural determination, crystals of compound 23-CdCl were collected under a microscope in 45% yield based on $CdCl_2$ and then washed, dried, and preserved in a vacuum. Anal. Calcd for 23-CdCl: C, 29.26; N, 6.83; H, 2.44. Found: C, 29.34; N, 6.85; H, 2.80. The typical Raman peaks belonging to Cd-Cl, C-H and N-H vibrations appear at 117 cm^{-1}, 1324 cm^{-1} and 3087 cm^{-1} respectively.

1.2 Synthesis of 23-ZnCl compound

$ZnCl_2$ (0.05 mmol) and HCl (3 mmol) were dissolved in mixed solution in H_2O (3 mL) and 2,3'-bipyridine (1 mL), and the mixture was then in a 25 mL round bottom flask reactor. The reactor was first heated at 80 °C for 3 hours and then slowly cooled to room temperature with a cooling rate of 5 °C·min^{-1}. After the filtration, block-shaped white crystals were obtained and subsequently determined as 23-ZnCl. After crystal structural determination, crystals of compound 23-ZnCl were collected under a microscope in 53% yield based on $ZnCl_2$ and then washed, dried, and preserved in a vacuum. Anal. Calcd for 23-ZnCl: C, 32.87; N, 7.67; H, 2.73. Found: C, 32.93; N, 7.65; H, 2.74.The typical Raman peaks belonging to Zn-Cl, C-H and N-H vibrations appear at 98 cm^{-1}, 1323 cm^{-1} and 3100 cm^{-1} respectively.

1.3 Synthesis of 23- $Cd_{0.5}Zn_{0.5}Cl$ compound

$CdCl_2$ (0.025 mmol), $ZnCl_2$ (0.025 mmol) and HCl (3 mmol) were dissolved in mixed solution in H_2O (3 mL) and 2,3'-bipyridine (1 mL), and the mixture was then in a 25 mL round bottom flask reactor. The reactor was first heated at 80 °C for 3 hours and then slowly cooled to room temperature with a cooling rate of 5 °C·min^{-1}. After the filtration, block-shaped white crystals were obtained and subsequently determined as 23-$Cd_{0.5}Zn_{0.5}Cl$. After crystal structural determination, crystals of compound 23-$Cd_{0.5}Zn_{0.5}Cl$ were collected under a microscope in 50% yield based on $ZnCl_2$ and then washed, dried, and preserved in a vacuum. As shown in Table S5, the ICPOES data indicated that real doping ratio of Cd^{2+} is 0.31 and the real doping ratio of Zn^{2+} is 0.69.

2. Characterization

2.1 Single-Crystal X-ray Diffraction (SCXRD)

Single-crystal X-ray diffraction data collection of all compounds were recorded using a Rigaku XtaLAB PRO II Advance instrumentation with graphitemonochromated Mo Kα (λ

= 0.78 Å) radiation. The crystalClear software package was used for data reduction and empirical absorption correction. The structure was solved by direct method using the SHELXL-97 and Olex 2 program. All nonhydrogen atoms were located by Fourier synthesis and the differential electron density function. The hydrogen atom coordinates were obtained by the difference electron density function combined with geometric analysis. All non-hydrogen atoms coordinate, and the anisotropy temperature factor, hydrogen atom coordinate, and isotropic temperature factor were corrected to convergence using full-matrix least-squares methods.

2.2 Powder X-ray Diffraction (PXRD)

The PXRD patterns were recorded on a Rigaku Miniflex 600 instrument with Cu Kα (λ = 1.54184 Å) radiation in the range of 10−60° at a scan rate of 8°/min.

2.3 ^{1}H NMR Titration

2,3'-bipyridine (10 mg, 9.79 × 10^{-6} mol) was dissolved in DMSO-d_6 (0.5 mL). Then, a series of different equivalents of **23-CdCl/23-ZnCl** (1.0, 2.0, 3.0, equiv and so on) were added into the solution of **23-CdCl/23-ZnCl**, and their ^{1}H NMRs were recorded.

2.4 Optical spectra measurement

The photoluminescence properties including the emission and excitation spectra in solid state were measured on a FLS980 Edinburgh fluorescence spectrometer. The PL quantum efficiency analysis was performed using the same light source with an additional integrating sphere. Time-resolved emission data were recorded at room temperature using the FLS980 spectrofluorometer. The dynamics of emission decay were monitored by using the FLS980s time-correlated single-photon counting capability with data collection for 10000 counts. Excitation was provided by an Edinburgh EPL-375 ps pulsed diode laser. The emission lifetime was obtained by single-exponential fitting.

2.5 Inductively Coupled Plasma Optical Emission Spectrometer (ICPOES)

ICP elemental analysis was carried out through a HORIBA Jobin Yvon Ultima2 instrument.

2.6 Thermogravimetric Analysis (TGA)

The thermogravimetric (TG) curves were measured on a Netzsch STA449C instrument heated from 30 to 800 °C at a ramp rate of 10.00°C/min, under a nitrogen flux of 100 mL min^{-1}.

2.7 Fourier Transform Infrared (FT-IR) Spectroscopy

The IR spectra were recorded on PerkinElmer Spectrum One spectrophotometer with KBr pellets in the range of 4000−400 cm^{-1}.

2.9 Elemental analyses (EA)

The EA of C, H, and N were carried out with a Vario EL III elemental analyzer.

2.9 Calculation details

All calculations in this study were based on density functional theory (DFT) using Gaussian 16 software, Revision A.03[1]. The single-point energy calculations for all the structures

involved in this paper were performed at the M06[2]/def2SVP[3] model, using the SMD[4] model with water as the solvent to take into account the solvation effect and with dispersion correction using GD3[5]. The Multiwfn[6] program was used to generate the fch files required for the NCI[7] analysis and visualized with the VMD[8] software.

3. Crystallographic Studies

3.1 Single Crystal Structure Determination of 23-CdCl

A colorless plank of 23-CdCl crystal with dimensions of 0.01 × 0.0275 × 0.0275 mm^3 was selected for single-crystal X-ray diffraction analysis. The diffraction data were collected on an Agilent Technologies SuperNova Dual Wavelength CCD diffractometer equipped with graphite-monochromated Mo Kα radiation (λ = 0.78 Å) at room temperature. The diffraction data were corrected for Lorentz and polarization factors as well as for absorption by multiscan method. The structure was solved by direct methods and refined by full-matrix least-squares fitting on SHELXL using the Olex 2 program package[9-11]. All atoms were refined with anisotropic thermal parameters. The structure was also checked for possible missing symmetry with PLATON. Crystallographic data and structural refinements are summarized in Table S1. Generally, the compound 23-CdCl, empirically formulated by structural determination as $(C_{10}H_{10}N_2)CdCl_4$, crystallizes in a trigonal system with space group Pbca and lattice parameters a = 7.5216(2) Å, b = 14.5647(3) Å, c = 26.7886(6) Å and Z = 8. The calculated density is 3.875 g/cm^3. The solution results are listed in Table S1-S2. CCDC 2295257 contains the supplementary crystallographic data for this paper. These data can be obtained free of charge from The Cambridge Crystallographic Data Centre via www.ccdc.cam.ac.uk/data_request/cif.

3.2 Single Crystal Structure Determination of 23-ZnCl

A colorless plank of 23-ZnCl crystal with dimensions of 0.01 × 0.025 × 0.025mm^3 was selected for single-crystal X-ray diffraction analysis. The diffraction data were collected on an Agilent Technologies SuperNova Dual Wavelength CCD diffractometer equipped with graphite-monochromated Mo Kα radiation (λ = 0.78 Å) at room temperature. The diffraction data were corrected for Lorentz and polarization factors as well as for absorption by multiscan method. The structure was solved by direct methods and refined by full-matrix least-squares fitting on SHELXL using the Olex 2 program package[9-11]. All atoms were refined with anisotropic thermal parameters. The structure was also checked for possible missing symmetry with PLATON. Crystallographic data and structural refinements are summarized in Table S1. Generally, the compound 23-ZnCl, empirically formulated by structural determination as $(C_{10}H_{10}N_2)ZnCl_4$, crystallizes in a trigonal system with space group Pbca and lattice parameters a = 12.2876(10) Å, b = 8.7564(7) Å, c = 12.3492(9) Å and Z = 4. The calculated density is 1.5 g/cm^3. The solution results are listed in Table S1, S3. CCDC 2295210 contains the supplementary crystallographic data for this paper. These data can be obtained free of charge from The Cambridge Crystallographic Data Centre via www.ccdc.cam.ac.uk/data_request/cif.

3.3 Single Crystal Structure Determination of 23-$Cd_{0.50}Zn_{0.50}Cl$ and 23-$Cd_{0.20}Zn_{0.80}Cl$

CCDC 2297733 and CCDC 2298043 contains the supplementary crystallographic data for this paper. These data can be obtained free of charge from The Cambridge Crystallographic Data Centre via www.ccdc.cam.ac.uk/data_request/cif.

4. Supplementary table and figures

Table S1 Single crystal X-ray diffraction data of 23-CdCl and 23-ZnCl.

Compound	**23-CdCl**	**23-ZnCl**
Formula	$(C_{10}H_{10}N_2)CdCl_4$	$(C_{10}H_{10}N_2)ZnCl_4$
Temperature	293 K	293 K
Space group	*Pbca*	*Pnma*
Volume	2934.69(12)	1328.71(18)
Unit cell dimensions	$a = 7.5216(2)$ Å	$a = 12.2876(10)$
	$b = 14.5647(3)$ Å	$b = 12.3492(9)$
	$c = 26.7886(6)$ Å	$c = 8.7564(7)$
	$\alpha = 90°$	$\alpha = 90°$
	$\beta = 90°$	$\beta = 90°$
	$\gamma = 90°$	$\gamma = 90°$
Z	8	4
ρ	3.875	1.5
Final R indexes [I>=2σ (I)]	$R_1 = 0.0247$,	$R_1 = 0.0429$,
	$wR_2 = 0.0557$	$wR_2 = 0.1273$
Final R indexes	$R_1 = 0.0340$,	$R_1 = 0.0518$,
[all data]	$wR_2 = 0.0591$	$wR_2 = 0.1327$

Table S2 Bond angles (°) for 23-CdCl single crystal.

Atom	Atom	Atom	Angle/°
Cl1	**Cd1**	**Cl2**	**107.515(22)**
Cl1	**Cd1**	**Cl3**	**107.363(26)**
Cl1	**Cd1**	**Cl4**	**109.577(22)**
Cl2	**Cd1**	**Cl3**	**108.504(24)**
Cl2	**Cd1**	**Cl4**	**108.080(25)**
Cl3	**Cd1**	**Cl4**	**115.531(24)**

Table S3 Bond angles (°) for 23-ZnCl single crystal.

Atom	Atom	Atom	Angle/°
Cl1	**Zn1**	**Cl2**	**117.647(149)**
Cl1	**Zn1**	**Cl3**	**109.601(132)**
Cl1	**Zn1**	**Cl4**	**107.031(115)**
Cl2	**Zn1**	**Cl3**	**109.292(108)**
Cl2	**Zn1**	**Cl4**	**106.829(660)**
Cl3	**Zn1**	**Cl4**	**105.850(114)**

Table S4. Hydrogen Bonds for **23-CdCl.**

D	H	A	d(D-H)/Å	d(H-A)/Å	d(D-A)/Å	D-H-A/°
C1	H1	Cl21	0.93	2.71	3.453(3)	137.9
C2	H2	Cl32	0.93	2.81	3.511(3)	133
C3	H3	Cl22	0.93	2.98	3.873(3)	160.5
C4	H4	Cl13	0.93	2.83	3.687(3)	153.3
C7	H7	Cl24	0.93	3.12	3.952(3)	149.1
C7	H7	Cl44	0.93	3.26	3.827(2)	121.4
C8	H8	Cl44	0.93	3.12	3.755(3)	127.2
C8	H8	Cl45	0.93	3.01	3.600(3)	122.6
C9	H9	Cl35	0.93	2.7	3.466(3)	139.9
C10	H10	Cl26	0.93	2.71	3.635(3)	173.6
N1	H1A	Cl1	0.86	2.28	3.108(2)	161
N2	H2A	Cl46	0.86	2.38	3.138(2)	146.7

Table S5. Hydrogen Bonds for **23-ZnCl**.

D	H	A	d(D-H)/Å	d(H-A)/Å	d(D-A)/Å	D-H-A/°
C1	**H1A**	**Cl21**	**0.93**	**3.02**	**3.622(5)**	**124**
C1	**H1A**	**Cl22**	**0.93**	**3.02**	**3.622(5)**	**124**
C2	**H2**	**Cl11**	**0.93**	**2.55**	**3.328(4)**	**141.3**
C2	**H2**	**Cl21**	**0.93**	**2.91**	**3.574(4)**	**129.8**
C6	**H6**	**Cl23**	**0.93**	**3**	**3.611(6)**	**124.8**
C6	**H6**	**Cl24**	**0.93**	**3**	**3.611(6)**	**124.8**

Table S6. Single crystal structure of hybrid organic–inorganic Zn/Cd halides.

Compound	PLE (nm)	PL (nm)	PLQY (%)	Dihedral Angle between aromatic rings (°)	Distance between aromatic rings (Å)	PL mechanism	Ref.
(P-xd)$ZnCl_4$	285	443	23.06	0.862	4.95	organic emission	12
(P-xd)$CdCl_4$	287	435	3.97	10.695	5.007	organic emission	12
R_2ZnCl_4	445	512	10.40	4.225	4.246	organic emission	13
R_2CdCl_4	453	528	11.21	10.337	4.664	organic emission	13
23-CdCl SCs	365	425, 560	11.7	0.117	3.898	organic emission	This work
23-$Cd_{0.5}Zn_{0.5}Cl$ SCs	365	425, 560	24.1	0.644	3.475	organic emission	This work
23-ZnCl SCs	365	425, 560	32.0	1.515	3.421	organic emission	This work
(H_2TTz)$ZnCl_4$·MeOH	365	462	18.00	11.001	4.1420	organic emission	14
(H_2TTz)$ZnBr_4$·MeOH	373	514	6.00	7.570	4.065	organic emission	14
$(PMA)_2ZnCl_4$	327	437, 496	37.2	2.807	4.211	organic emission and STEs	15
$(PBA)_2ZnCl_4$	353	446, 478	14.2	1.117	5.52	organic emission and STEs	15
($TpyH_3$)[$ZnCl_4$]-[Cl] (Tpy-Zn)	430	490	24.13	5.213	3.639	organic emission and STEs	16
($TpyH_3$)[$CdCl_4$]-[Cl] (Tpy-Cd)	430	490	25.67	4.519	3.894	organic emission and STEs	16

Table S7. ICPOES data of 23-$Cd_{0.90}Zn_{0.10}Cl$, 23-$Cd_{0.80}Zn_{0.20}Cl$, 23-$Cd_{0.50}Zn_{0.50}Cl$ and 23-$Cd_{0.30}Zn_{0.70}Cl$.

Crystal	Element	Reaction adding ratio	Real doping ratio
23-$Cd_{0.90}Zn_{0.10}Cl$	Cd	0.90	0.85
	Zn	0.10	0.15
23-$Cd_{0.80}Zn_{0.20}Cl$	Cd	0.80	0.70
	Zn	0.20	0.30
23-$Cd_{0.50}Zn_{0.50}Cl$	Cd	0.50	0.31
	Zn	0.50	0.69
23-$Cd_{0.30}Zn_{0.70}Cl$	Cd	0.30	0.17
	Zn	0.70	0.83

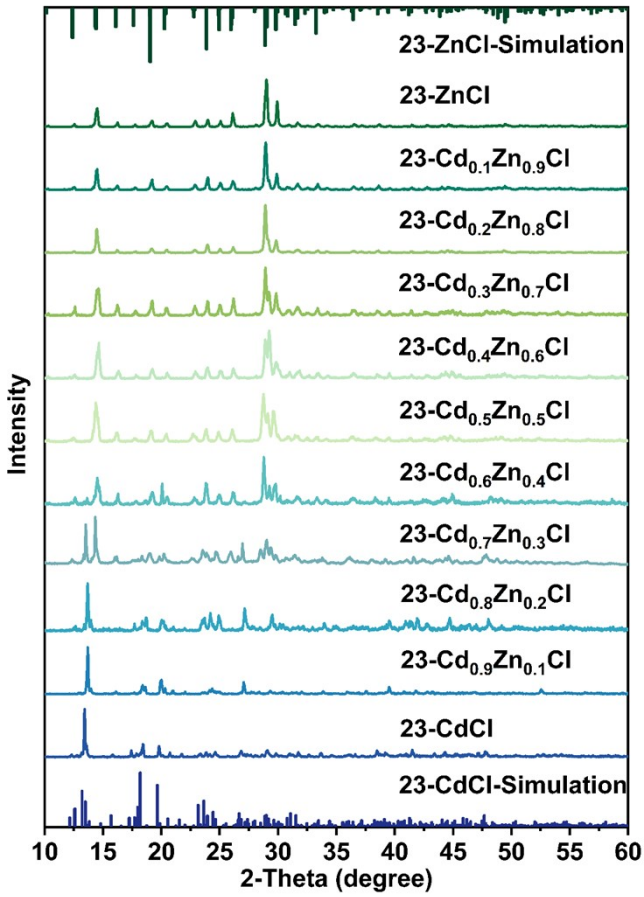

Figure S1. Powder XRD pattern of 23-$Cd_{1-x}Zn_xCl$ (x= 0.1, 0.2, …, 1) crystals powder.

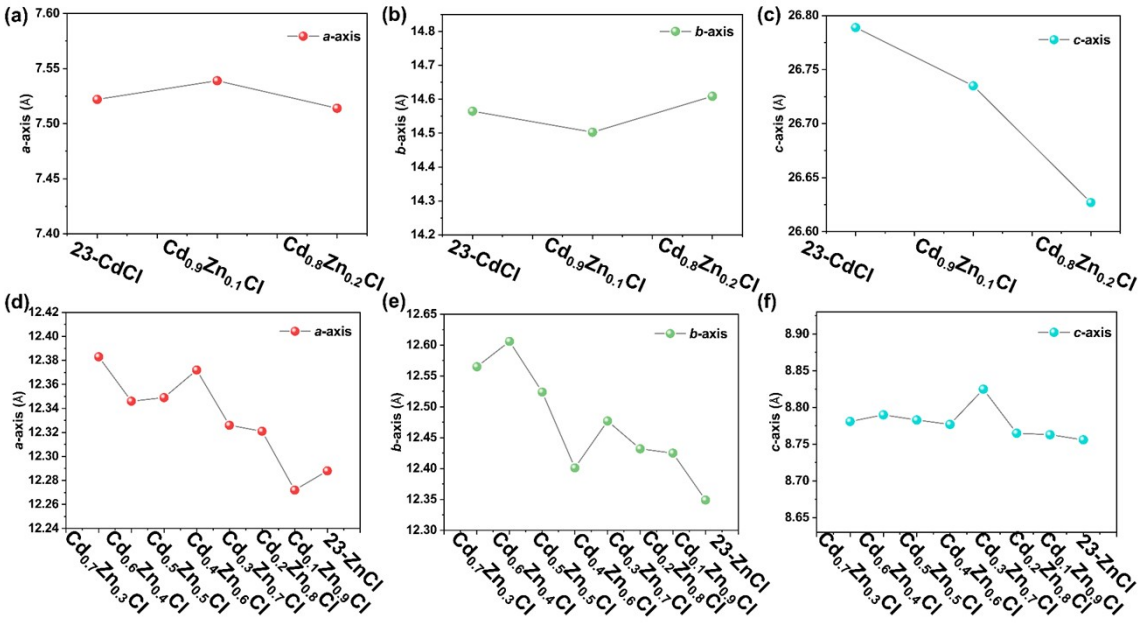

Figure S2. Composition dependent cell lengths of 23-$Cd_{1-x}Zn_xCl$ (x = 0.1, 0.2, …, 1) crystal (Note: two phases of 23-CdCl and 23-ZnCl co-exist when x =0.3 and 0.4, only the cell lengths of the component isostructural with 23-CdCl phase is displayed when x =0.3 and 0.4).

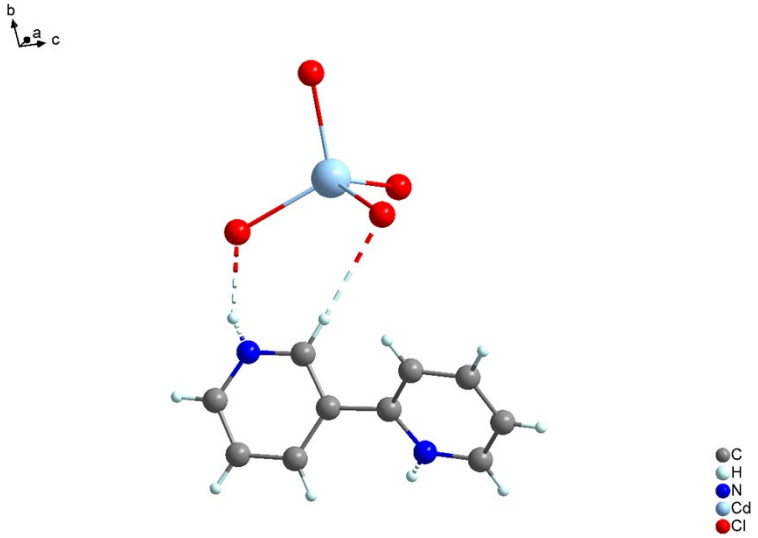

Figure S3. Asymmetric unit of 23-CdCl crystal.

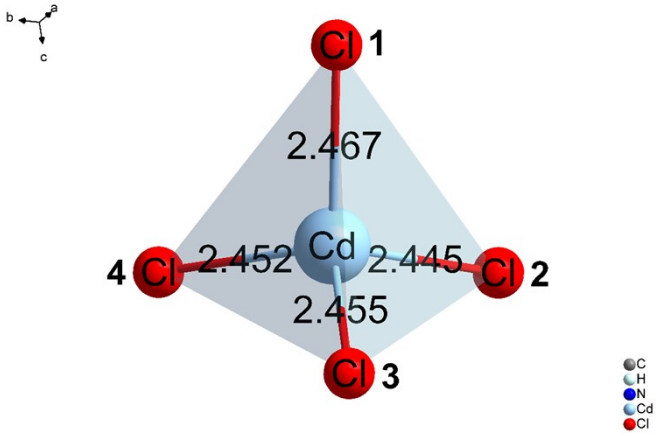

Figure S4. Coordination mode of Cd^{2+}.

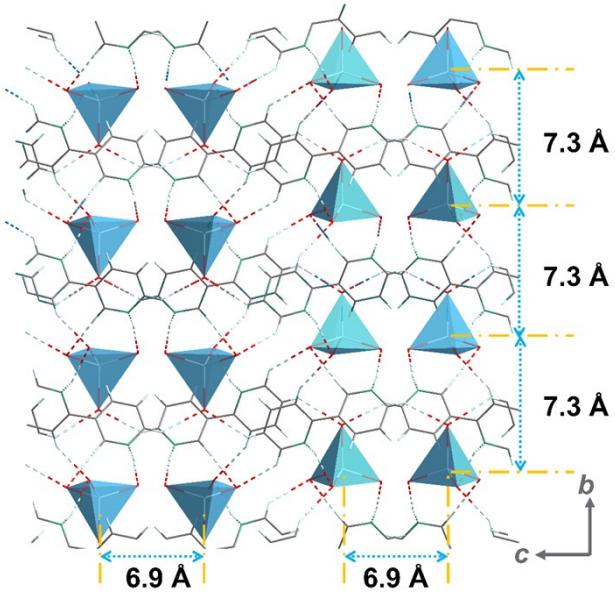

Figure S5. Crystal structure of 23-CdCl viewed along the *a* axis.

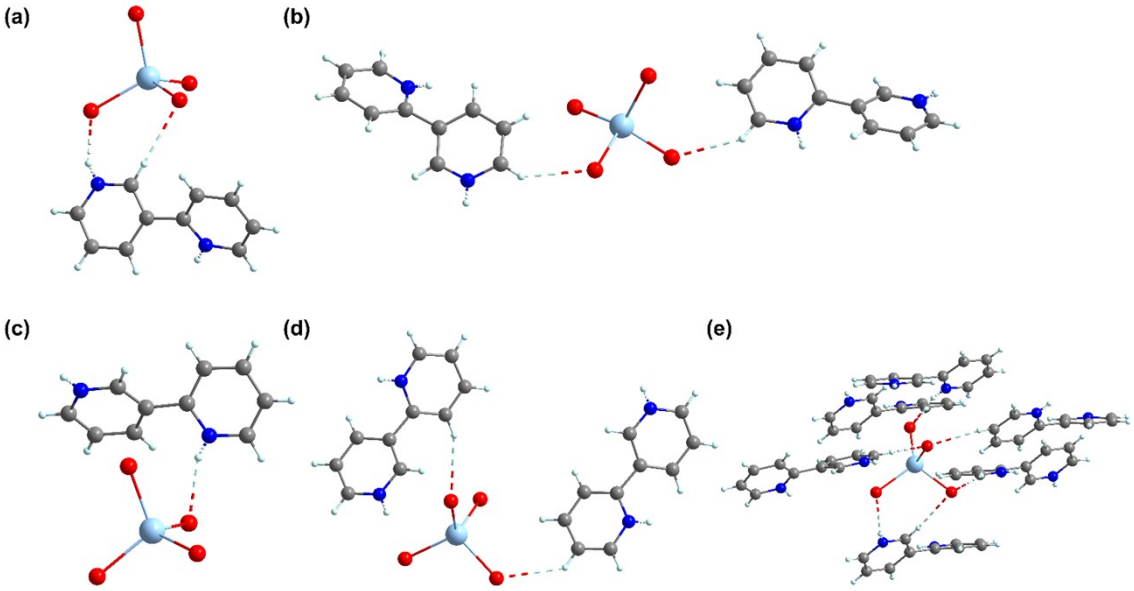

Figure S6. Coordination mode of $[CdCl_4]^{2-}$.

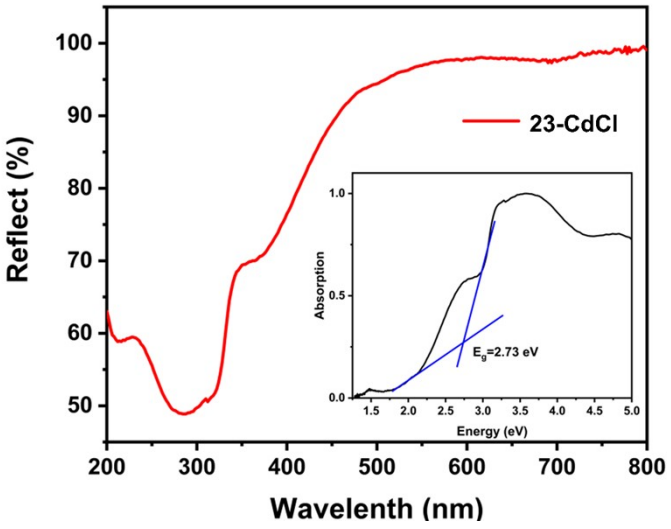

Figure S7**.** Diffuse reflection spectrum of **23-CdCl** crystals powder.

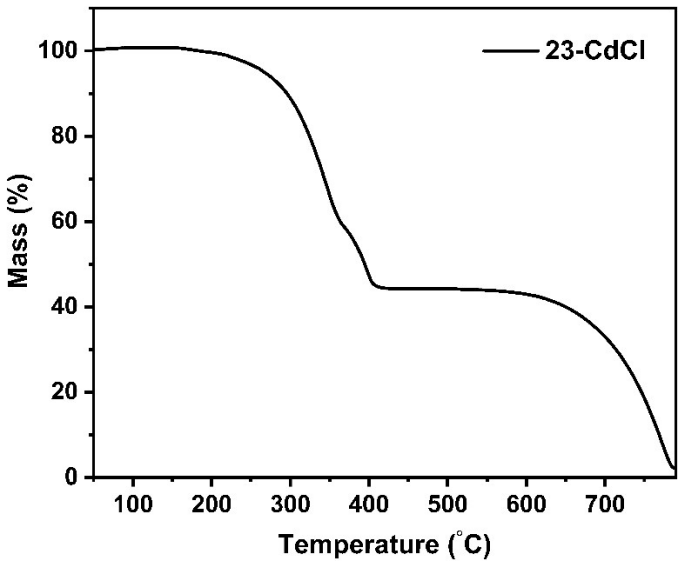

Figure S8. TGA curve of 23-CdCl.

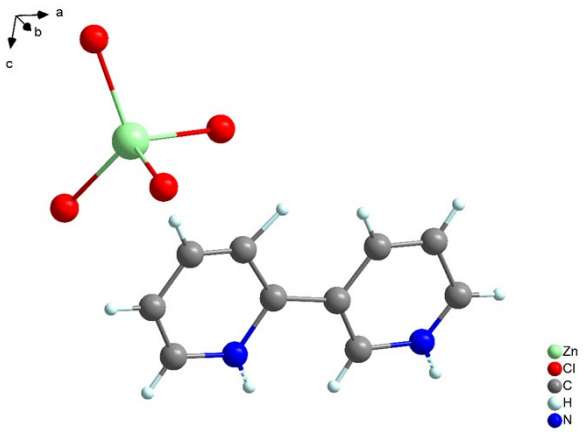

Figure S9. Asymmetric unit of 23-ZnCl crystal.

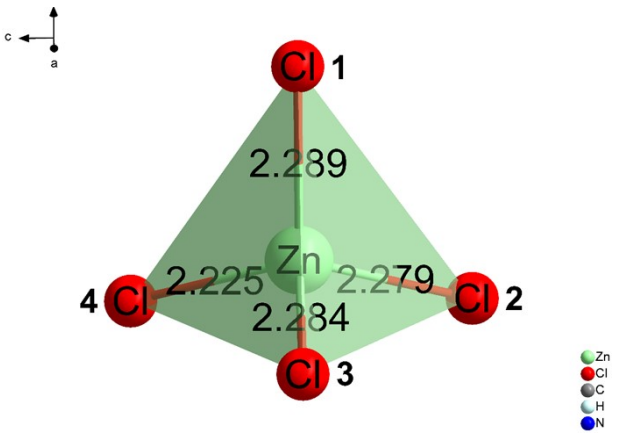

Figure S10. Coordination mode of Zn^{2+}.

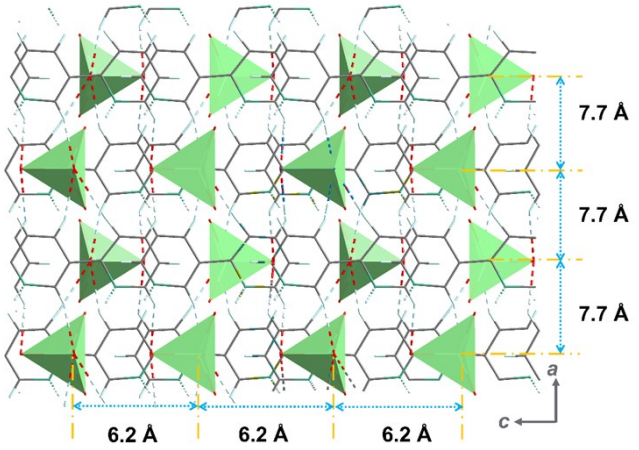

Figure S11. Crystal structure of 23-ZnCl viewed along the *b* axis.

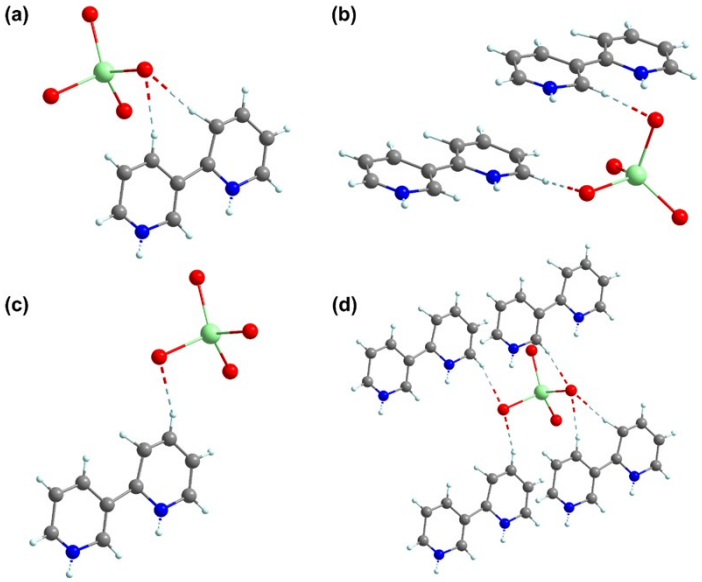

Figure S12. Coordination mode of $[ZnCl_4]^{2-}$.

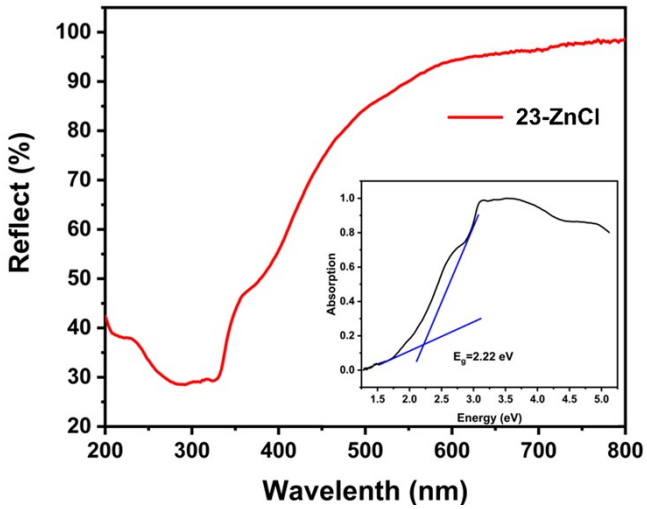

Figure S13**.** Diffuse reflection spectrum of **23-ZnCl** crystals powder.

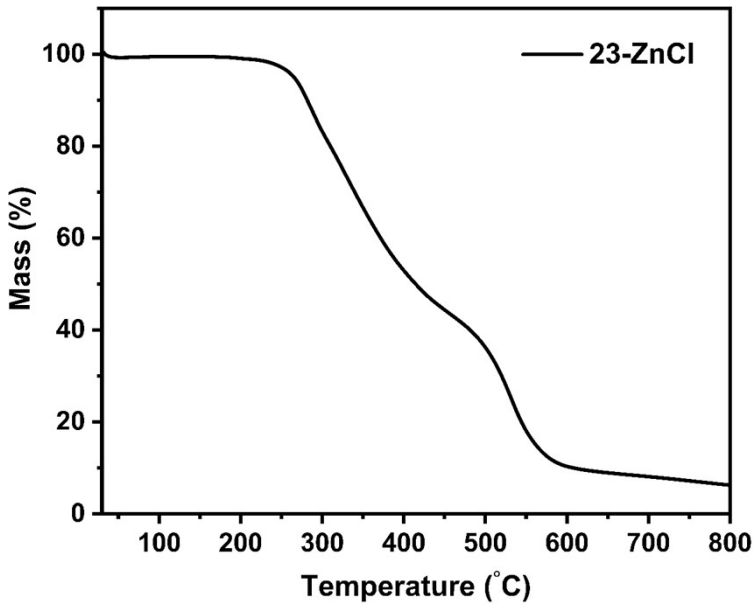

Figure S14. TGA curve of 23-ZnCl.

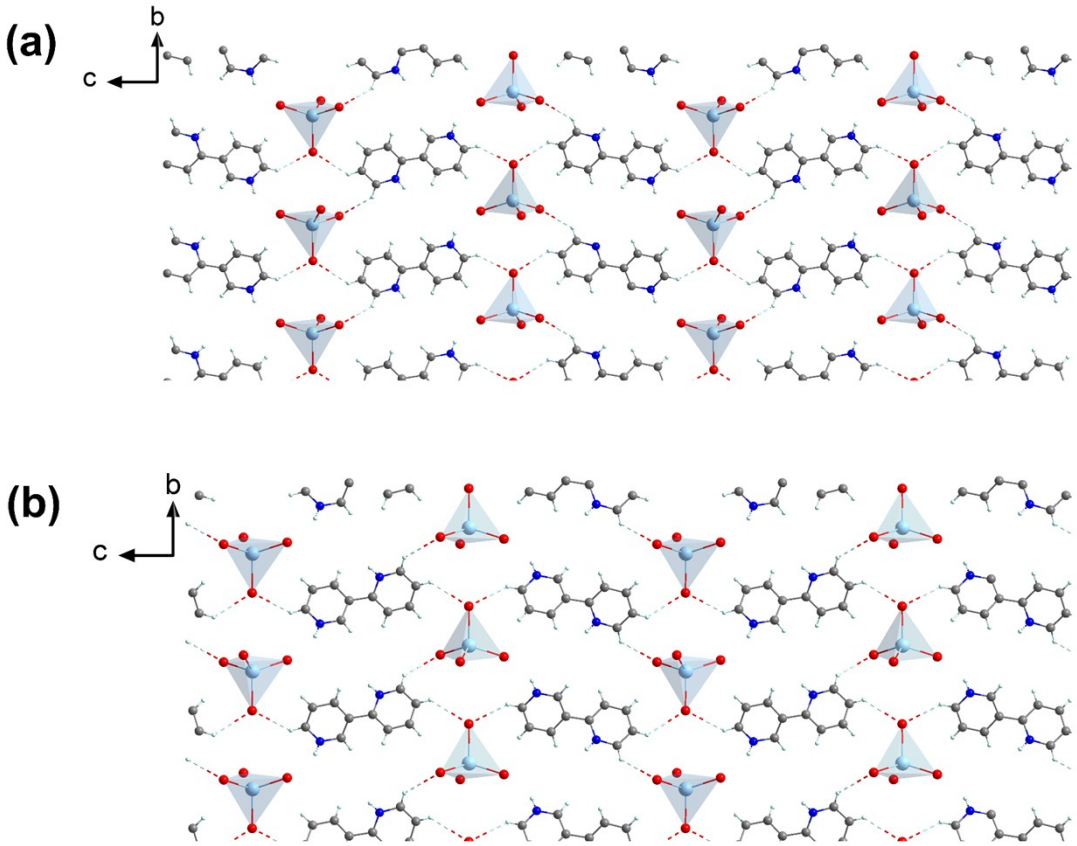

Figure S15. Structure of the 23-CdCl SCs: layer A (a) and layer B (b).

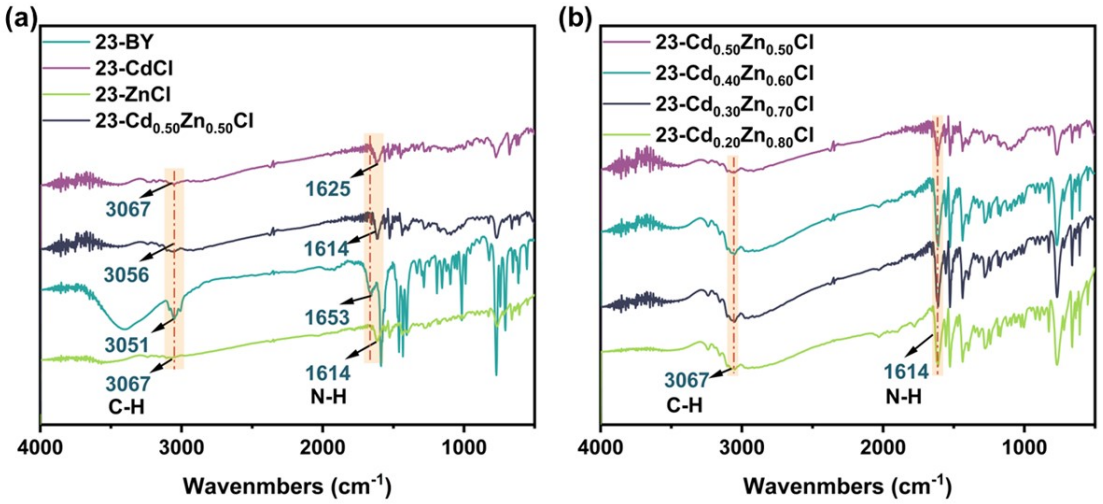

Figure S16. (a) FT-IR spectra of the **2,3'-bipyridine, 23-CdCl, 23-ZnCl** and **23-$Cd_{0.5}Zn_{0.5}Cl$.** (b) FT-IR spectra of the **23-$Cd_{0.5}Zn_{0.5}Cl$, 23-$Cd_{0.4}Zn_{0.6}Cl$, 23-$Cd_{0.3}Zn_{0.7}Cl$** and **23-$Cd_{0.2}Zn_{0.8}Cl$**.

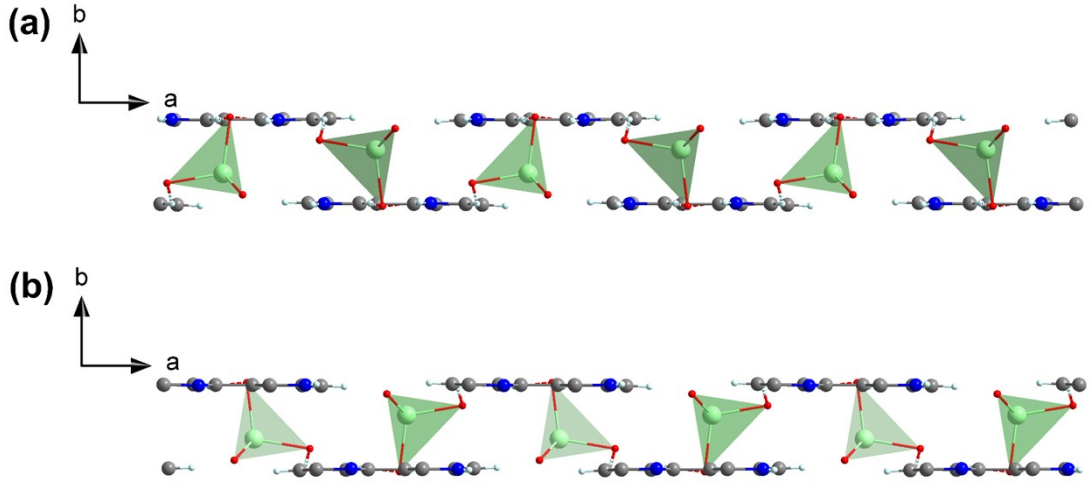

Figure S17. Structure of the 23-ZnCl SCs: layer A (a) and layer B (b).

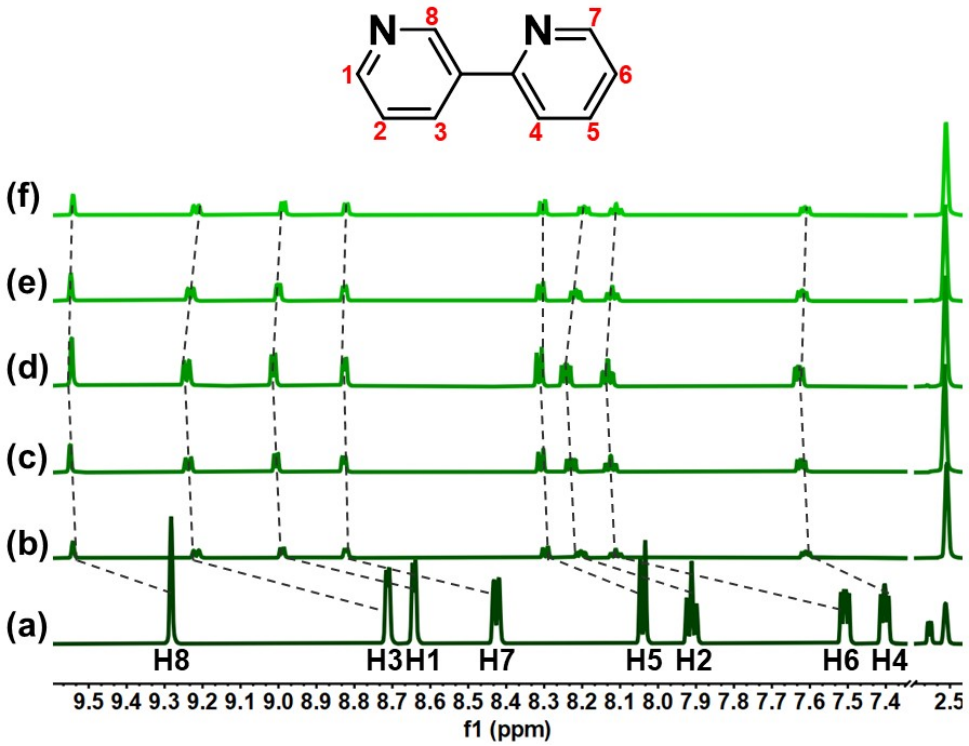

Figure S18**.** Partial ^{1}H NMR spectra of various equivalents of **23-CdCl** (DMSO-d_6): (a) the free **2,3'-bipyridine,** (b) **23-CdCl** 1.0 equiv, (c) **23-CdCl** 2.0 equiv , (d) **23-CdCl** 3.0 equiv , (e) **23-$Cd_{0.5}Zn_{0.5}Cl$** 1.0 equiv , (f) **23-ZnCl** 1.0 equiv.

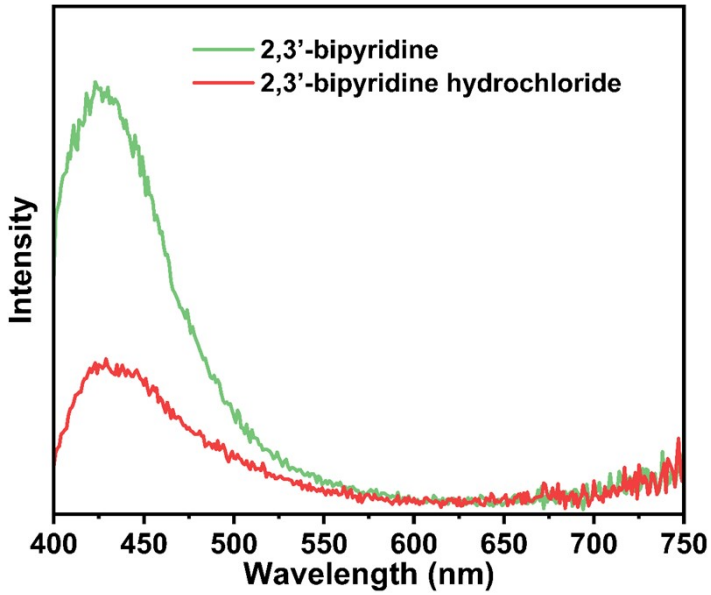

Figure S19**.** Photoluminescence spectra of **2,3'-bipyridine and 2,3'-bipyridine hydrochloride** (at 365 nm).

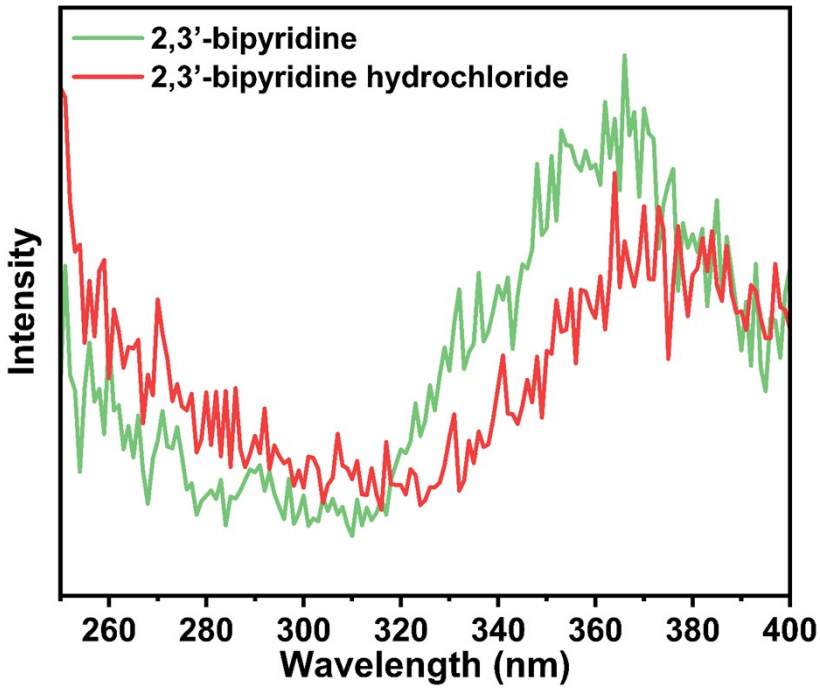

Figure S20**.** Excitation spectra of **2,3'-bipyridine and 2,3'-bipyridine hydrochloride** (at 425nm excitation).

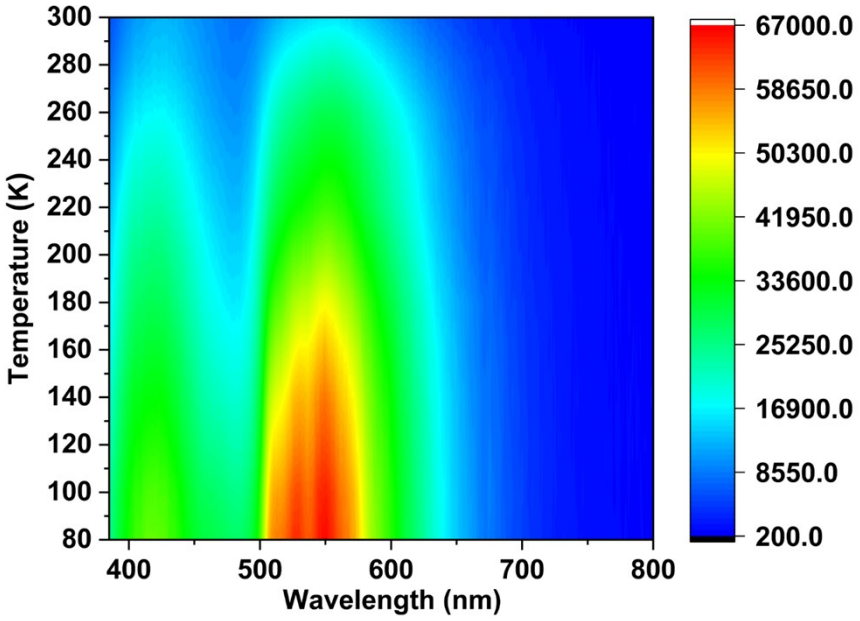

Figure S21**.** Temperature dependent photoluminescence spectra of 23-$Cd_{0.50}Zn_{0.50}Cl$.

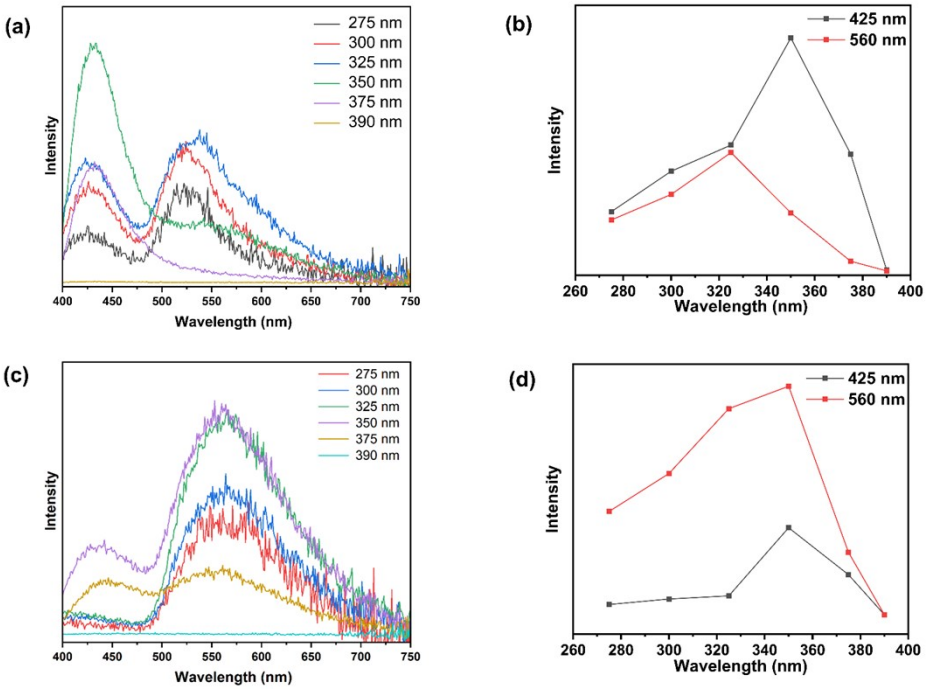

Figure S22. Excitation-wavelength dependent PL spectra of 23-CdCl at RT (a), comparison of PL intensity at 425nm and 560nm of 23-CdCl (b), Excitation-wavelength dependent PL spectra of 23-ZnCl at RT (c) and comparison of PL intensity at 425nm and 560nm of 23-ZnCl (d).

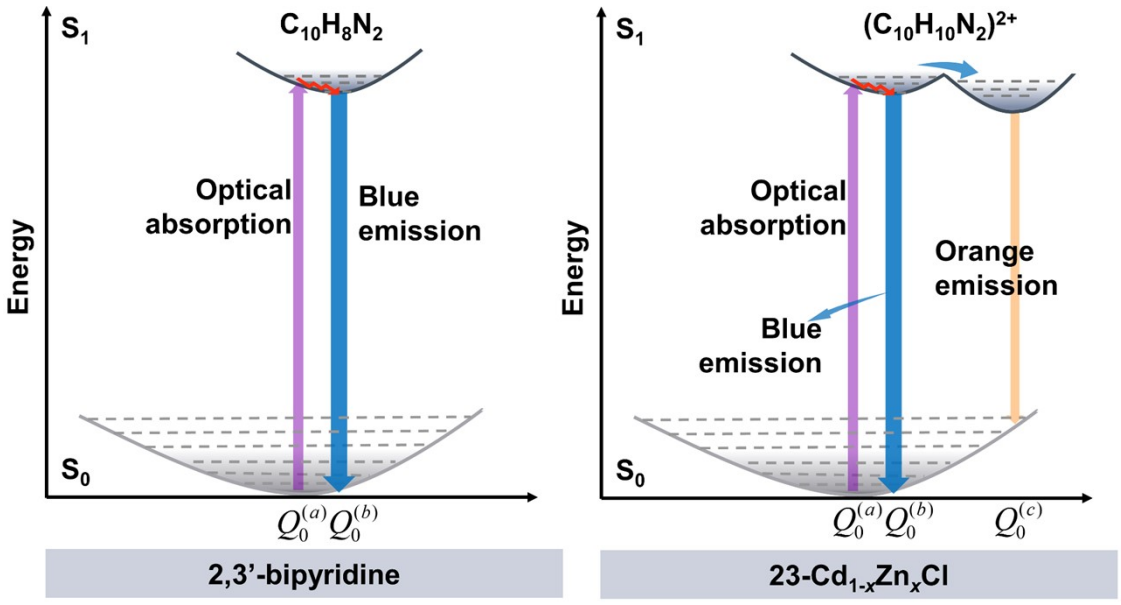

Figure S23. Scheme of the photo luminescence dynamic of 2,3'-bipyridine and 23-$Cd_{1-x}Zn_xCl$ crystals.

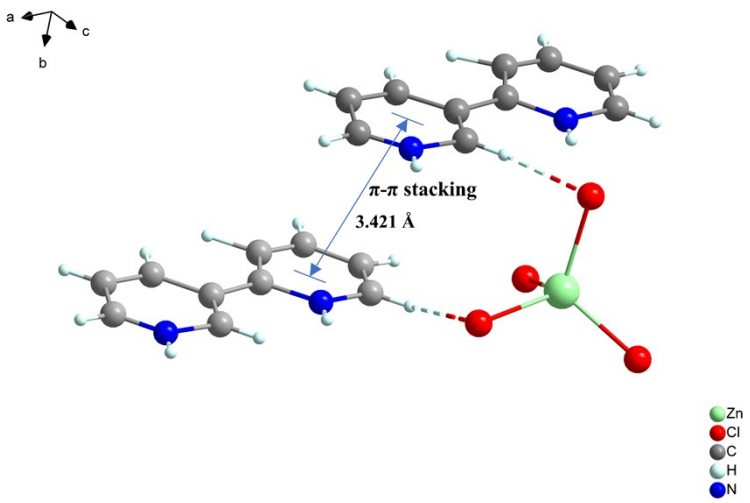

Figure S24. Details of the π-π stacking between 2,3'-bipyridinium cations in 23-ZnCl crystal.

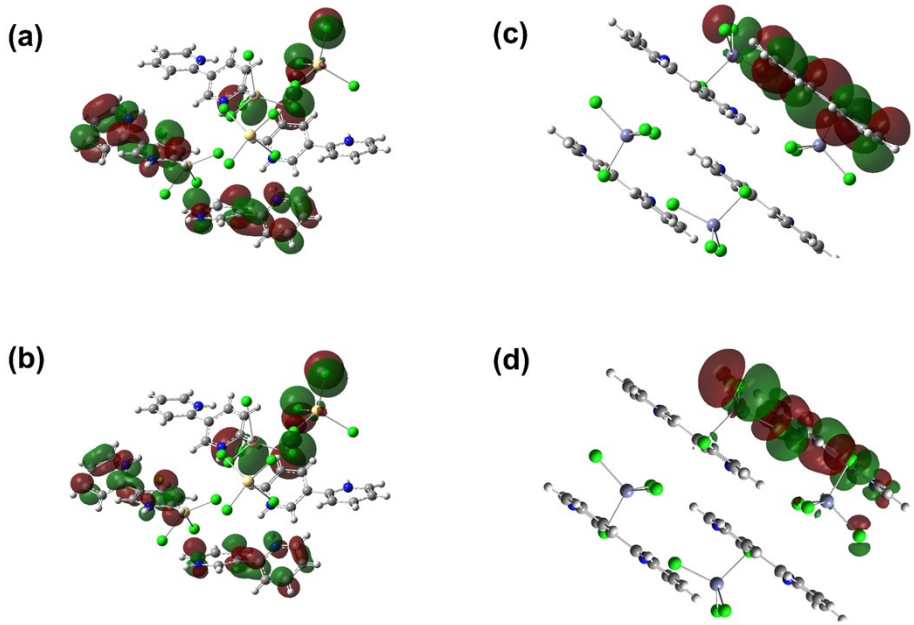

Figure S25. Calculated **HOMO-LUMO** of 23-CdCl (a, b) and 23-ZnCl (c, d).

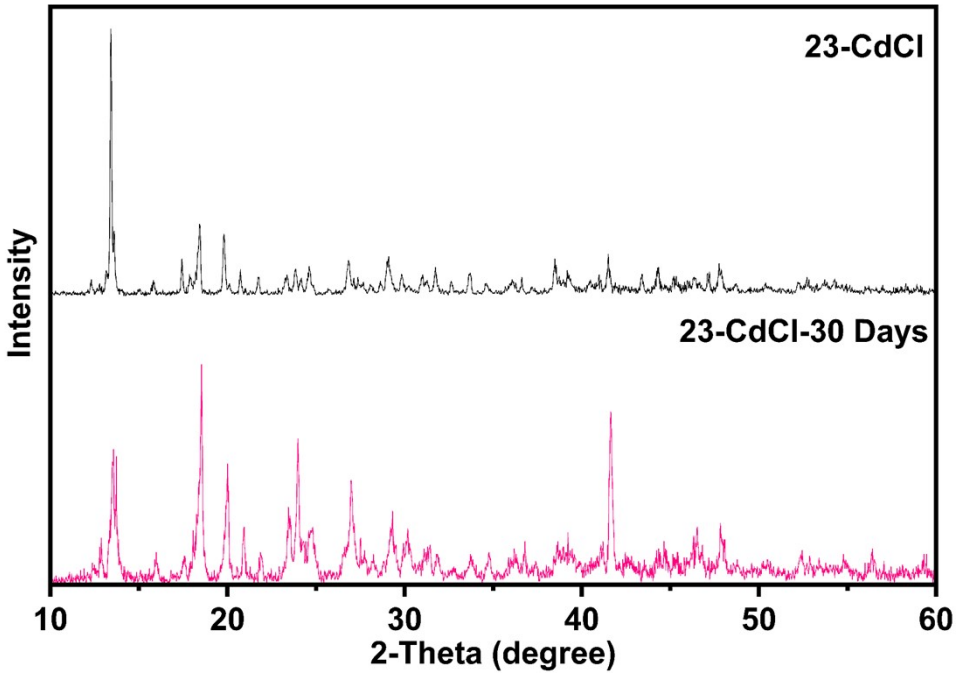

Figure S26. Experimental PXRD patterns of 23-CdCl after storage in moist air for 30 Days.

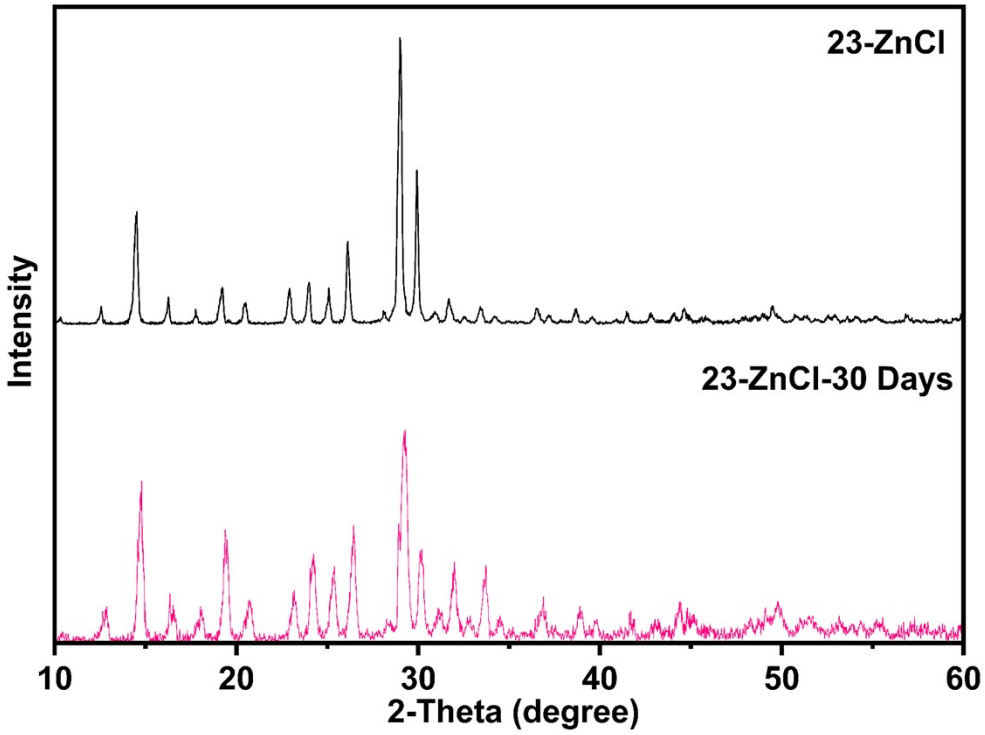

Figure S27. Experimental PXRD patterns of 23-ZnCl after storage in moist air for 30 Days.

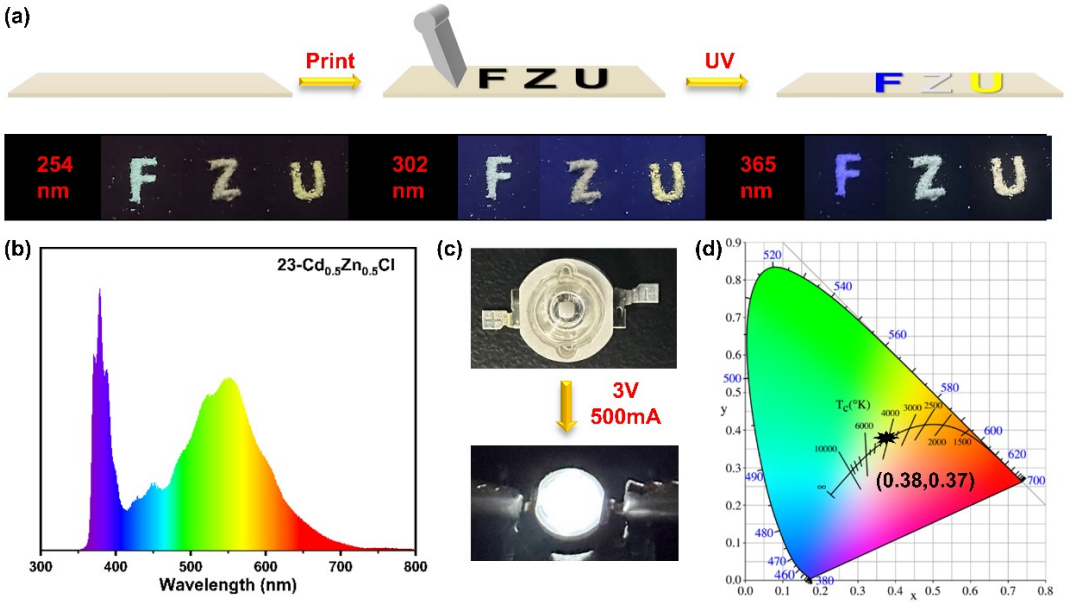

Figure S28. (a) Schematic diagram of screen printing 23-$Cd_{0.5}Zn_{0.5}Cl$. (b-d) Schematic diagram and characterization of electroluminescent diodes.

5.References

[1] Gaussian 16, Revision A.03, M. J. Frisch, G. W. Trucks, H. B. Schlegel, G. E. Scuseria, M. A. Robb, J. R. Cheeseman, G. Scalmani, V. Barone, G. A. Petersson, H. Nakatsuji, X. Li, M. Caricato, A. V. Marenich, J. Bloino, B. G. Janesko, R. Gomperts, B. Mennucci, H. P. Hratchian, J. V. Ortiz, A. F. Izmaylov, J. L. Sonnenberg, D. Williams-Young, F. Ding, F. Lipparini, F. Egidi, J. Goings, B. Peng, A. Petrone, T. Henderson, D. Ranasinghe, V. G. Zakrzewski, J. Gao, N. Rega, G. Zheng, W. Liang, M. Hada, M. Ehara, K. Toyota, R. Fukuda, J. Hasegawa, M. Ishida, T. Nakajima, Y. Honda, O. Kitao, H. Nakai, T. Vreven, K. Throssell, J. A. Montgomery, Jr., J. E. Peralta, F. Ogliaro, M. J. Bearpark, J. J. Heyd, E. N. Brothers, K. N. Kudin, V. N. Staroverov, T. A. Keith, R. Kobayashi, J. Normand, K. Raghavachari, A. P. Rendell, J. C. Burant, S. S. Iyengar, J. Tomasi, M. Cossi, J. M. Millam, M. Klene, C. Adamo, R. Cammi, J. W. Ochterski, R. L. Martin, K. Morokuma, O. Farkas, J. B. Foresman, and D. J. Fox, Gaussian, Inc., Wallingford CT, 2016.

[2] Zhao Y, Truhlar D G. The M06 suite of density functionals for main group thermochemistry, thermochemical kinetics, noncovalent interactions, excited states, and transition elements: two new functionals and systematic testing of four M06-class functionals and 12 other functional[J]. Theor. Chem. Acc., 2008, 120: 215-241.

[3] Schäfer A, Horn H, Ahlrichs R. Fully optimized contracted Gaussian basis sets for atoms Li to Kr[J]. The Journal of Chemical Physics, 1992, 97(4): 2571-2577.

[4] A.V. Marenich, C.J. Cramer, D.G. Truhlar, Universal solvation model based on solute electron density and on a continuum model of the solvent defined by the

bulkdielectric constant and atomic surface tensions, J. Phys. Chem. B 113 (2009) 6378–6396.
[5] Grimme S, Antony J, Ehrlich S, et al. A consistent and accurate ab initio parametrization of density functional dispersion correction (DFT-D) for the 94 elements H-Pu[J]. The Journal of chemical physics, 2010, 132(15): 154104.
[6] Lu T, Chen F W. Multiwfn: A multifunctional wavefunction analyzer [J]. J. Comput. Chem., 2012, 33: 580-592.
[7] Johnson, E. R.; Keinan, S.; Mori-Sanchez, P.; Contreras Garcia, J.; Cohen, A. J.; Yang, W. Revealing noncovalent interactions. J. Am. Chem. Soc. 2010, 132, 6498-6506.
[8] Humphrey W, Dalke A, Schulten K. VMD: visual molecular dynamics [J]. Journal of Molecular Graphics, 1996, 14: 33-38.
[9] Sheldrick, G. M. Crystal structure refinement with SHELXL. Acta Crystallogr., Sect. C: Struct. Chem. 2015, 71, 3−8.
[10] Sheldrick, G. M. A short history of SHELX. Acta Crystallogr., Sect. A: Found. Crystallogr. 2008, 64, 112−122.
[11] Dolomanov, O.V.; Bourhis, L.J.; Gildea, R.J.; Howard, J.A.K.; Puschmann, H., OLEX2: A complete structure solution, refinement and analysis program (2009). J. Appl. Cryst., 42, 339-341.
[12] D.A. Popy, B.N. Evans, J. Jiang, T.D. Creason, D. Banerjee, L.M. Loftus, R. Pachte, D.T. Glatzhofer and B. Saparov, Mater. Today Chem. 2023, 30, 101502.
[13] Creason, T. D., Fattal, H., Gilley, I. W., Evans, B. N., Jiang, J., Pachter, R., Glatzhofer, D. T., Saparov, B., Inorg. Chem. Front. 2022,9, 6202.
[14] Li, K.-J., Zhao, Y.-Y., Sun, M.-E., Chen, G.-S., Zhang, C., Liu, H.-L., Li, H.-Y., Zang, S.-Q., Mak, T. C. W., Cryst. Growth Des. 2022, 22, 3295.
[15] S. He, S. Hao, L. Fan, K. Liu, C. Cai, C. Wolverton, J. Zhao and Q. Liu, Adv. Optical Mater. 2023, 11, 2300218.
[16] S. Wang, Z. Liang, X. Song, X. Huang, L. Liu, X. Jiang, Z. Lin and H. Liu, Inorg. Chem. 2023, 62, 21451.